Vibroacoustic Investigation of Light-Weight Ceilings - Modeling aspects and Design Guidelines

M. Buchschmid, M. Kohrmann, G. Müller
Lehrstuhl für Baumechanik, Technische Universität München, 80333 München, Deutschland.

U. Schanda
Fakultät für angewandte Natur- und Geisteswissenschaften, Hochschule für angewandte Wissenschaften Rosenheim, 83024 Rosenheim, Deutschland.

Summary

In order to set up guidelines for the design of light-weighted ceilings for timber constructions, investigations based on both measurements and numerical models have been carried out in the research project "'VibWood"' an TU München and HAW Rosenheim [5]. A semi-analytical approach for the prediction of radiated sound is presented, which is based on Integral Transform Methods. The method can be applied in the post-processing of a Finite-Element-computation. Thus as a first step the structure, consisting of a cross laminated timber ceiling with floating floor and suspended ceiling, is build-up in a Finite-Element-model, where the material properties of wood and the characteristics of the system are considered. The model is parameterized to enable computations with varying geometry and material parameters and calibrated with measurements using model-updating-techniques. The model for the air in the cavity of the suspended ceiling is discussed, where a FSI-model with acoustic fluid elements is compared against simplified engineering approaches.

PACS no. 02.30.Uu, 02.70.Dh, 47.11.Fg, 43.40.At, 43.50.Cb

1. Introduction

Nowadays a trend towards using wooden constructions in multi-story buildings for industrial as well as for residential use is recognizable. This can be explained by reasons of profitability and of course by the necessity to develop sustainable engineering concepts. The serviceability linked with vibrations is a key issue for such light-weighted structures especially for timber slabs. In particular in a frequency range beneath 100 Hz these structures are prone to pedestrian induced vibrations, footfall noise as well as re-radiated sound caused by induced vibrations (see Figure 1).

To investigate this phenomenon an AiF sponsored research project named "VibWood" has been established. It is carried out by the Chair of Structural Mechanics at the Technische Universität München (TUM) and University of Applied Sciences Rosenheim. The overall goal of the project is to develop guidelines to describe the acoustical and dynamical behavior of wooden ceilings and to design adapted

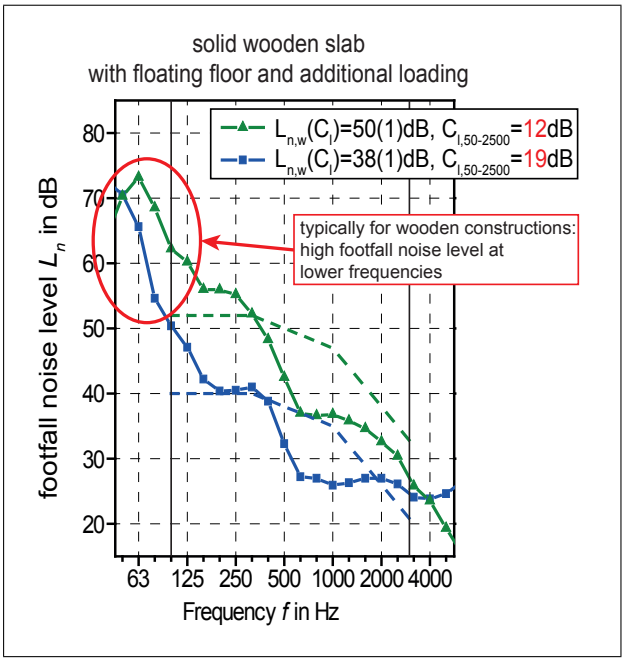

Figure 1. Standard footfall noise level

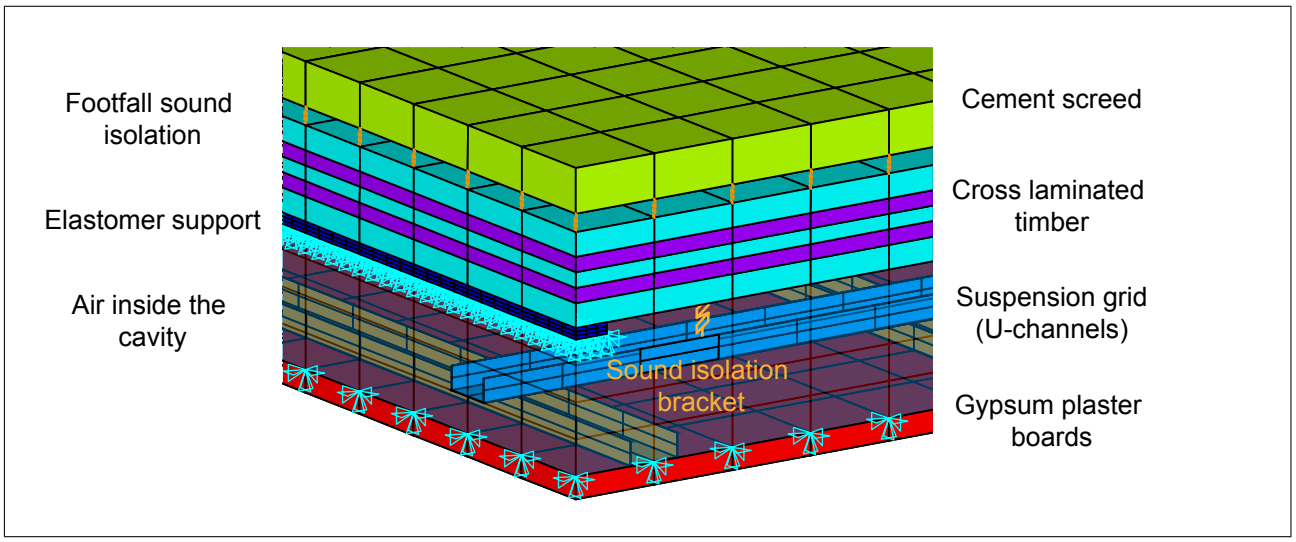

Figure 2. FE model of a cross laminated timber slab with suspended ceiling and floating foor

protection systems regarding vibrations. At the testing lab in Rosenheim a measurement based investigation of the vibro-acoustical characteristics of three different timber floors (timber beam, cross laminated timber and hollow-box) with suspended ceilings or floating floors is performed. These results are used to calibrate the corresponding numerical models developed by TUM to predict the sound radiation behavior of multiple geometrical parameter combinations by numerical simulations. Figure 2 shows a characteristic FE model of a cross laminated timber ceiling in the final construction state.

This contribution is dealing with aspects of numerical modeling and model updating of a plane cross laminated timber ceiling, modeling of the air cavity inside a suspended ceiling and the prediction and dimensional analysis of the radiated sound power. Therefore the initial numerical model has to be developed adequately with respect to material parameters according to the specific characteristics of wood as an orthotropic material, contact parameters for adjusting the coupling and support conditions as well as the geometrical parameters. These parameters will be calibrated using experimental data with a geometrical parameter combination according to the testing structure. With the calibrated model it will be possible to run simulations of multiple sets of geometrical parameter combinations. The results are summarized in nomograms with dimensionless parameters which are developed with a dimensional analysis.

2. Prediction of the structural vibrations

2.1. Numerical Model

Before starting to develop numerical models it is essential to have a closer look at the testing structure. The testing structure is a five-layered cross laminated timber slab with a length and a width of 5.5 m and a thickness of 105 mm. It consists of four separated plates that are longitudinally coupled with screwed embedded laminated veneer lumber boards. The whole floor is line supported on two sides with L-shaped steel profiles that are directly attached to the concrete floor of the testing lab. To prevent a lifting of the structure steel U-channels are used to fix the slab to the support. In between elastomer stripes have been arranged to create properly defined support conditions.

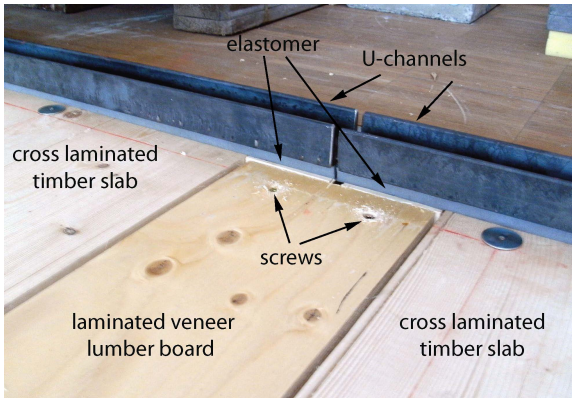

Figure 3. Details of the coupling and support conditions

Starting with one set of geometrical parameters the material properties are investigated. As wood is an orthotropic material its elasticity tensor is generally depending on nine material parameters: *Young*'s modulus, shear modulus and *Poisson* ratio for longitudinal, radial and tangential direction. In the special case of wood the tangential and radial direction can be summarized as a perpendicular direction by taking into account that the cutting direction of the wooden

boards is varying. That means there are six material properties left for the parallel (longitudinal) and the perpendicular direction. The density of the slab has been measured by weighting and is not subject to further investigations. The material properties and especially in this case the coupling and support conditions have to be modeled in such a way that they reproduce the testing structure [4].

For the coupling of the neighboring plates a substitute system has to be developed to replace the laminated veneer lumber connection. Therefore all displacements of the coincident nodes of the top line of the top layer elements of each plate were coupled while their rotation remained unconstrained. To prevent large element distortions the coincident bottom line nodes of the top layer-elements were also constrained except for the displacement in y-direction. This degree of freedom was coupled with one-dimensional spring elements, introducing the spring stiffness $k_{y,lin}$ as a new parameter.

The remaining point of interest regarding the numerical model are the support conditions. As mentioned before a minor complex construction using U-shaped steel profiles and elastomer stripes was applied, multiple numerical experiments have shown that a substitute system just consisting of a single elastomer stripe properly fixed to the cross laminated timber model was suitable. To take into account the small cross-section of the elastomer stripes they have to be modeled with element sizes much smaller than the slabs mesh size. To couple the displacements of both structures constraint equations at the interface were applied using an implemented function of the Finite-Element software ANSYS®. The elastomer's *Young*'s modulus E_{syl} completes the set of unknown model parameters.

2.2. Model-Updating

In the last section an appropriate parametric numerical model of a cross laminated timber slab was presented which shall be calibrated with respect to eight unknown material and coupling parameters $E_{\parallel}$, $E_{\perp}$, $G_{\parallel\perp}$, $G_{\perp\perp}$, $\nu_{\parallel\perp}$, $\nu_{\perp\perp}$, $k_{y,lin}$ and E_{syl}. Thus a model updating based on experimental data is performed for a set of geometrical parameters according to the testing structure.

For the model updating in a first step an objective function is defined, which takes the systems Eigen frequencies into account. To update the overall behavior of the model in the investigated frequency range the root mean square of the variance of simulated and measured Eigen frequencies was chosen. Its lowest possible value is the objective of the model updating process.

$$f(x) = \sqrt{\frac{1}{k}\sum_{i=1}^{k}\left(\frac{f_{a,i}(x) - f_{m,i}}{f_{m,i}} \cdot 100\right)^2} \qquad (1)$$

Table I. Model-Updating results

Parameters		Initial values	Final values
$E_{\perp}$	Nmm^2	400	137
$G_{\parallel\perp}$	$\frac{\mathrm{N}}{\mathrm{mm}^2}$	550	459
$G_{\perp\perp}$	$\frac{\mathrm{N}}{\mathrm{mm}^2}$	80	74.2
$E_{x,Syl}$	$\frac{\mathrm{N}}{\mathrm{mm}^2}$	13	11.3
$k_{y,lin}$	N	10	10.1
$\nu_{\parallel\perp}$	–	0.07	0.052
RMS value with initial values			7.32 %
RMS value after the optimization			5.01 %

To get simulated Eigen frequencies the results of a numerical modal analysis were used. The experimental data required intensive measurements in the testing lab. There an Experimental Modal Analysis (EMA) was performed based on the slabs transfer functions, which were generated by a forced shaker excitation and the answering signal of 144 acceleration transducers [3].

The sequence for the updating algorithm was chosen as follows: First the parameters of the numerical model are changed and a numerical simulation is started based on starting values chosen in advance. For the solution a modal analysis is performed resulting in the model's Eigen mode shapes and Eigen frequencies. Before these Eigen frequencies can be combined with the measurement data based on the EMA the matching Eigen frequencies have to be evaluated. For this reason the corresponding simulated and measured Eigen mode shapes are investigated using the Modal Assurance Criterion (MAC).

$$\mathbf{MAC}_{jk} = \frac{\left|\Phi_{mj}^T \Phi_{sk}\right|^2}{(\Phi_{mj}^T \Phi_{mj})(\Phi_{sk}^T \Phi_{sk})} \qquad (2)$$

With the matching Eigen frequencies the objective function can be evaluated for the specific parameter combination. Taking the result into account, depending on the used algorithm the sequence starts anew with a changed set of parameters. In a first step a starting configuration was found by a grid search to find the global minimum and avoid local minima. In a second step a steepest descent algorithm was carried out. Table I shows the initial parameters found by a grid search and the final parameters after the updating process. The final values result in an root mean square variance value of 5.01 %. $\nu_{\perp\perp}$ was found to have no influence on the system's Eigen modes and was neglected.

2.3. Dimensional Analysis

The numerical models have been calibrated for one set of geometrical parameters. A prediction of the characteristics of cross laminated timber slabs of varying

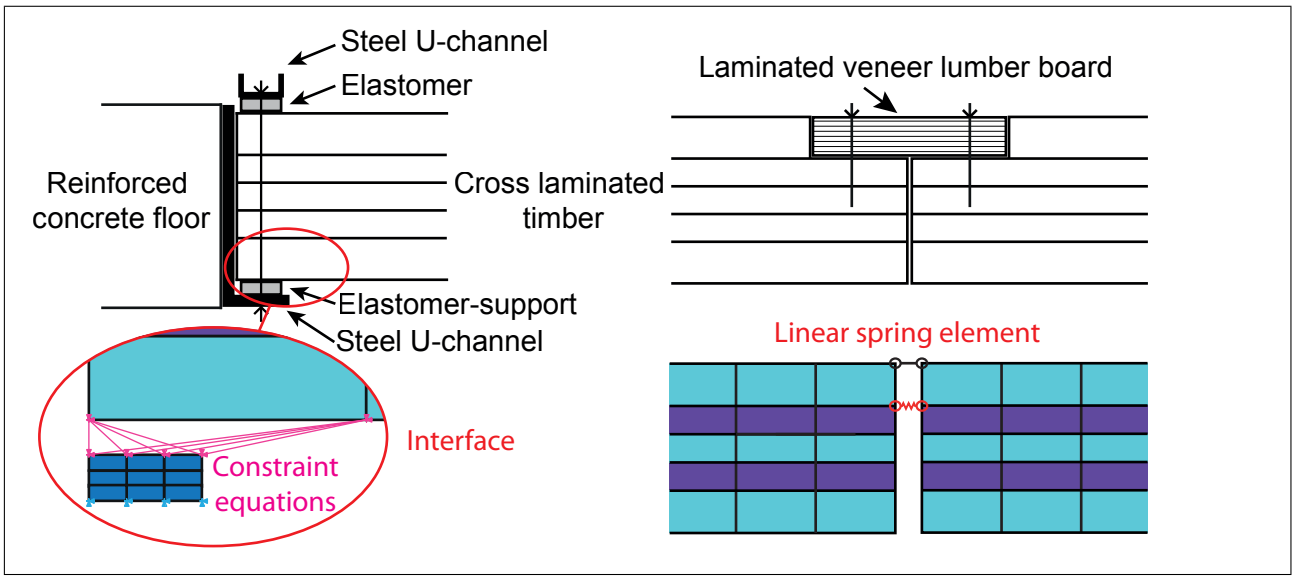

Figure 4. Modeling of support conditions and connections

geometry is now possible, however, it is necessary to find an appropriate way for a clear illustration of the results. The presented approach is based on the Buckingham π-Theorem which states that physical laws describing the functional relation between the physical parameters must be independent of the chosen unit system. Out of the given parameters Q a number of free parameters Q_r has to be chosen that corresponds to the number of independent physical units. The remaining now bonded parameters Q_k are expressed as dimensionless parameters π_k by dividing them by a specific power product of the free parameters.

$$\pi_k = \frac{Q_k}{Q_1^{a_{1k}} \cdot Q_i^{a_{ik}} \cdot \ldots \cdot Q_r^{a_{rk}}} \quad \text{where} \quad [\pi_k] = 1 \tag{3}$$

Running a large number of simulations changing mass, stiffness, length and widths and also the number of the plates, the results could be presented in a dimensionless form in order to draw conclusions. In figure 5 the results for the radiated sound power are shown for all sets of parameters. Comparing the results in detail (which should not be discussed in this contribution) principles can be derived for each type of structure. E.g. with constant span the number of individual segments orthogonal to the span of the plates (ratio of length and width) have just a small influence on the sound radiation. Varying the thickness however one observes a high sensitivity regarding the sound radiation [2][5].

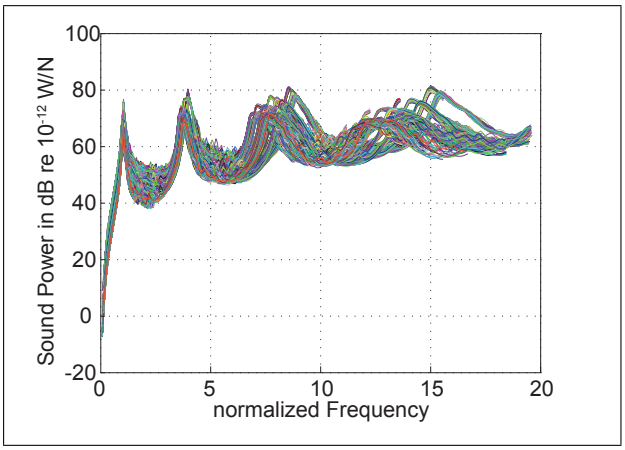

Figure 5. Sound power results of the parametric study for cross laminated timber ceilings

3. Sound radiation of plates - computation in the Fourier-domain

3.1. Theoretical aspects

The sound radiation can be computed as a closed form solution modeling the radiating surface within an infinite (reflective) surface as depicted in [1][6]. The velocity field $v = v(x, y, \Omega)$ at the surface of the radiator is obtained from a numerical analysis e.g. using a finite element model or from measurements. For ideal plates it can be modeled as a sum of plane waves and evanescent fields. With the help of a twofold Fourier-transformation from the spatial into the wave number domain the spectral decomposition of the velocity field is obtained.

$$\hat{v}(k_x, k_y, \Omega) = \int_{-\infty}^{+\infty} \int_{-\infty}^{+\infty} v(x, y, \Omega) e^{-ik_x x} e^{-ik_y y} dx dy \tag{4}$$

Here Ω is the angular frequency of excitation, k_x and k_y are the wave numbers according to the coordinates x and y. The combination of k_x and k_y results in a wavenumber k_r related to an oblique wave:

$$k_r = \sqrt{k_x^2 + k_y^2}. \tag{5}$$

For ideal plates with large dimensions compared to the bending wave length the wavenumber k_r corresponds to the bending wave.

Integrating over an infinite x-y-plane for $z = 0$ (interface between structure and acoustic fluid) the velocity at the area outside the radiator is set to $v = 0$.

The steady state sound pressure in the room is also defined in the domain of the Fourier transformed variables, the wavenumbers and the angular frequency of excitation:

$$p(x, y, z, t) = \hat{p}(k_x, k_y, \Omega) e^{-ik_x x} e^{-ik_y y} e^{-ik_z z} e^{i\Omega t} \tag{6}$$

$p(x, y, z, t)$ fulfills the wave equation

$$\frac{\partial^2 p}{\partial x^2} + \frac{\partial^2 p}{\partial y^2} + \frac{\partial^2 p}{\partial z^2} - \frac{\partial^2 p}{c_A^2 \partial t^2} = 0\,, \tag{7}$$

if $k_z = \sqrt{k_A^2 - k_x^2 - k_y^2} = \sqrt{k_A^2 - k_B^2}$. Here c_A marks the speed of sound in the acoustic fluid, $k_A = \frac{\Omega}{c_A}$ is the corresponding wave number and k_B is the resulting wave number used for the coupling with the radiating surface.

In the following the exponential functions are abbreviated with $E = e^{-ik_x x} e^{-ik_y y} e^{-ik_z z} e^{i\Omega t}$. At the interface between acoustic fluid and radiating surface ($z = 0$) the normal component of the velocity v_z in the air is equated with the velocity v of the plate. According to Newton's law

$$\nabla p = -\rho_A \frac{\partial v}{\partial t} \tag{8}$$

where $\nabla = \frac{\partial}{\partial x} e_x + \frac{\partial}{\partial y} e_y + \frac{\partial}{\partial z} e_z$ marks the nabla operator and ρ_A is the density of the acoustic fluid this boundary condition leads to the following expression:

$$v_{z=0} = \frac{-1}{i\Omega\rho_A} \frac{\partial p}{\partial z}\bigg|_{z=0} = \frac{k_z\, \hat{p}(k_x, k_y, \Omega)}{\Omega \rho_A} E\bigg|_{z=0} \tag{9}$$

The quantities $\hat{p}(k_x, k_y, \Omega)$ and $\hat{v}(k_x, k_y, \Omega)$ are abbreviated by $\hat{p}$ and $\hat{v}$ in the following.

The amplitude $\hat{p}$ for the sound pressure is obtained from equation (9) for each combination of wave numbers and frequency:

$$\hat{p} = \frac{\Omega \rho_A}{k_z} \hat{v} = \rho_A c_A \frac{k_A}{k_z} \hat{v} \tag{10}$$

Finally the sound pressure in the space domain can be computed by the inverse transformation (superposition of the spectral components):

$$p(x, y, z, \Omega) = \frac{\rho_A c_A}{4\pi^2} \int_{-\infty}^{+\infty} \int_{-\infty}^{+\infty} \frac{k_A}{k_z}\, \hat{v}\, E\, \mathrm{d}k_x \mathrm{d}k_y \tag{11}$$

In order to compare different setups of plates the influence of the adjacent room is not considered. The sound power of a plane radiator with the area A into an infinite domain is computed as follows:

$$P(\Omega) = \frac{1}{2} \Re \iint_{(A)} p\, v^* \mathrm{d}A \tag{12}$$

Conjugate complex values are marked with * in the following. The velocity field in the air can be computed from equation (4) for a harmonic excitation:

$$v = \frac{1}{4\pi^2} \int_{-\infty}^{+\infty} \int_{-\infty}^{+\infty} \hat{v}\, E\, \mathrm{d}k_x \mathrm{d}k_y \tag{13}$$

Inserting the equations for sound pressure (11) and sound velocity (13) into equation (12), integrating over the area A and simplifying the expressions, according to [6], the radiated sound power is computed depending on $\hat{v}$, k_A and k_B:

$$P(\Omega) = \frac{1}{2} \frac{\rho_A c_A}{4\pi^2} \Re \int_{-\infty}^{+\infty} \int_{-\infty}^{+\infty} \frac{k_A}{\sqrt{{k_A}^2 - {k_B}^2}}\, \hat{v}\, \hat{v}^* \mathrm{d}k_x \mathrm{d}k_y \tag{14}$$

In equation (14) the sound power is described by the real part $\Re$ of the integral's result. Hence only wave numbers contribute to the sound power for which the value $\sqrt{{k_A}^2 - {k_B}^2}$ is real. After discretization of the analytical integral the radiated sound power of a plane radiator can be computed numerically with the help of discrete values:

$$P(\Omega) = \frac{1}{2} \frac{\rho_A c_A}{4\pi^2} \Re \left[\sum_{n_x} \sum_{n_y} \frac{k_A}{k_z}\, \hat{v}\, \hat{v}^*\, \Delta k_x \Delta k_y \right]. \tag{15}$$

3.2. Validation with measurements

In Figure 6 the transfer function of the sound power level is plotted for two different methods. The light blue curve represents the results out of the intensity measurement which is used as a reference solution. Predicting the radiated sound pressure out of the velocity pattern of the suspended ceiling by ITM-Postprocessing the blue curve results. A good agreement to the reference solution is observed. The gray section indicates the frequency range where the intensity measurements produce no valid results.

4. Air inside the cavity

The last point of interest is the modeling of the air inside the cavity of the suspended ceiling. The structural model consists of gypsum plaster boards (shell

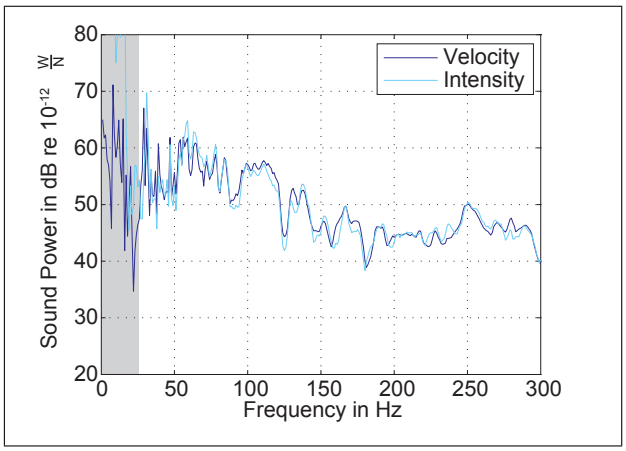

Figure 6. Transfer function of the sound power level: Intensity measurement with pp-probe vs. velocity measurement postprocessed by ITM

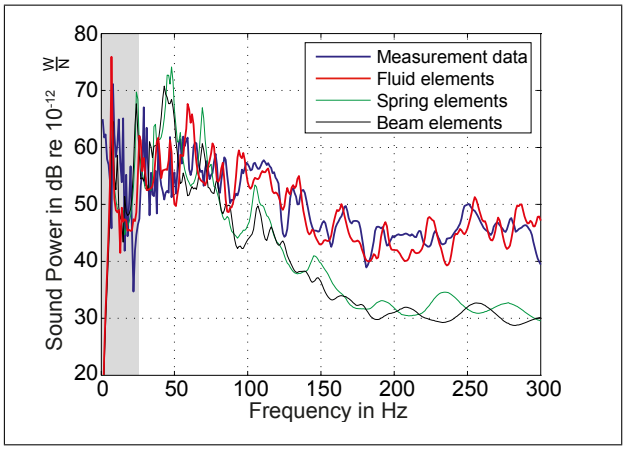

Figure 7. Transfer function of the sound power level: Measurement data vs. simulated data using fluid spring and beam elements for the modeling of the air in the cavity

elements) that are mounted onto a grid of steel U-channels (beam elements) suspended by sound isolation brackets (spring-damper elements) as shown in figure 2. The material parameters have been evaluated by experimental modal analyses.

For the modeling of the air approaches with air substituted by either vertical spring or beam elements between main ceiling and gypsum plaster boards are compared to a model with acoustical fluid elements that leads to significant increase in computational effort. Figure 7 shows the resulting radiated sound power of all models compared to measurement data. Only the acoustic fluids produce results with a good correlation whereas the radiated sound power of the simplified models is up to 20 dB lower in the frequency range above approximately 60 Hz. As described in [5] this is due to the fact that the transmission of the vibrational energy is mainly depending on the air's eigen modes which the simplified models cannot cover.

5. CONCLUSIONS

This contribution has shown that many different aspects have to be taken into account to develop adequate numerical models. Especially when parametric models are required the parameters must be chosen appropriately and the parameters must be calibrated by measurement results. Using Integral Transform Techniques the prediction of the radiated sound can be carried out efficiently out of the velocity field of a vibrating ceiling, obtained out of a FEM computation. A dimensionless approach is well suited to develop nomograms that describe the structure's radiated sound power. Finally models of the air inside the suspended ceiling were discussed. It was shown that the use of acoustical fluid elements is necessary whereas simplified engineering models lead to incorrect results.

Acknowledgement

The IGF project 16758 N of the iVtH (Internationaler Verein für technische Holzfragen e.V.) was supported by the AIF (Allianz Industrie Forschung) within the framework of the promotion of Industrial Research, funded by the German Ministry of economy and technology. Technical support was provided by Müller-BBM VibroAkustik Systeme GmbH.

References

[1] M. Kohrmann, M. Buchschmid, R. Völtl, G. Müller, U. Schanda: Prognose von sekundärem Luftschall bei leichten Geschossdeckensystemen mit Integraltransformationsmethoden. Proc. DAGA 2012

[2] M. Kohrmann, M. Buchschmid, A. Greim, G. Müller, U. Schanda: Vibroacoustic Characteristics of light-weighted Slabs - Part 1: Aspects of Numerical Modeling, Model Updating and Parametric Studies using the Buckingham-π-Theorem. Proc. AIA-DAGA 2013

[3] M. Buchschmid, C. Winter, M. Kohrmann, R. Völtl, G. Müller, U. Schanda: Vibroacoustic Characteristics of light-weighted Slabs - Part 2: Measurement-Based Investigation of the Sound Radiation of Suspended Ceilings. Proc. AIA-DAGA 2013

[4] M. Kohrmann, M. Buchschmid, G. Müller, R. Völtl, U. Schanda: Numerical models for the prediction of vibro-acoustical characteristics of light-weighted ceilings. Proc. Internoise 2013

[5] M. Kohrmann, R. Völtl, M. Buchschmid, G. Müller, U. Schanda: Planungshilfen zur schall- und schwingungstechnischen Beschreibung von Holzdecken und zur Bewertung und Dimensionierung von angepassten Schwingungsschutzsystemen - AiF Research Project "VibWood". Tech. Rept. Technische Universität München, Hochschule für angewandte Wissenschaften Rosenheim, 2014

[6] L. Cremer, M. Heckl, B.A.T. Petersson: Structure Borne Sound. Springer. 2005